

A Novel Multi-objective Physiological Control System for Rotary Left Ventricular Assist Devices

Journal Article**Author(s):**

Petrou, Anastasios; Monn, Marcial; Meboldt, Mirko; [Schmid Daners, Marianne](#) 

Publication date:

2017-12

Permanent link:

<https://doi.org/10.3929/ethz-b-000184520>

Rights / license:

[In Copyright - Non-Commercial Use Permitted](#)

Originally published in:

Annals of Biomedical Engineering 45(12), <https://doi.org/10.1007/s10439-017-1919-0>

A Novel Multi-objective Physiological Control System for Rotary Left Ventricular Assist Devices

ANASTASIOS PETROU, MARCIAL MONN, MIRKO MEBOLDT, and MARIANNE SCHMID DANERS

Department of Mechanical and Process Engineering, Product Development Group Zurich, ETH Zurich, CLA G 21.1, Tannenstrasse 3, 8092 Zurich, Switzerland

(Received 20 June 2017; accepted 6 September 2017; published online 12 September 2017)

Associate Editor Umberto Morbiducci oversaw the review of this article.

Abstract—Various control and monitoring algorithms have been proposed to improve the left-ventricular assist device (LVAD) therapy by reducing the still-occurring adverse events. We developed a novel multi-objective physiological control system that relies on the pump inlet pressure (PIP). Signal-processing algorithms have been implemented to extract the required features from the PIP. These features then serve for meeting various objectives: pump flow adaptation to the perfusion requirements, aortic valve opening for a predefined time, augmentation of the aortic pulse pressure, and monitoring of the LV pre- and afterload conditions as well as the cardiac rhythm. Controllers were also implemented to ensure a safe operation and prevent LV suction, overload, and pump backflow. The performance of the control system was evaluated *in vitro*, under preload, afterload and contractility variations. The pump flow adapted in a physiological manner, following the preload changes, while the aortic pulse pressure yielded a threefold increase compared to a constant-speed operation. The status of the aortic valve was detected with an overall accuracy of 86% and was controlled as desired. The proposed system showed its potential for a safe physiological response to varying perfusion requirements that reduces the risk of myocardial atrophy and offers important hemodynamic indices for patient monitoring during LVAD therapy.

Keywords—Hybrid mock circulation, Pressure sensor, Aortic valve opening control, Suction, Overload, Backflow, Monitoring, Pulsatile speed modulation, Physiological control.

INTRODUCTION

Rotary left-ventricular assist devices (LVADs) have been established as a viable treatment method for heart failure (HF), the leading health problem in developed

countries. Despite several decades of development and significant technological improvements,²⁹ LVADs are still associated with life-threatening adverse events, such as pump thrombosis and gastrointestinal bleeding.¹⁵ The constant-speed operation of the clinical LVADs is assumed to be one of the factors that induces some of these adverse events. Operating an LVAD at constant speed may lead to non-physiological and critical blood flow conditions, such as LV suction and overload due to over- and underpumping, respectively, and in the long term may result in adverse events such as right-ventricular failure and pulmonary edema.³²

In clinical practice, no feedback controllers have been implemented to prevent these critical flow conditions. However, some companies have incorporated in their devices feedforward controllers that detect suction, based on the estimated or measured pump flow, and release it by decreasing the pump speed to a predefined setpoint. Additionally, they have implemented algorithms to enable an aortic valve opening or to augment the aortic pulse pressure of the patients. Despite those algorithms, it is believed that a more physiological behavior of an LVAD can be achieved to presumably reduce some of the adverse events and improve the LVAD therapy. For this purpose, the research has focused for many years on the development of such algorithms.^{11,18–20,26,32}

A number of monitoring^{11,18–20} and control algorithms³² have been proposed to monitor the condition of the patient and generate a physiological pump flow. For monitoring, there exist algorithms that focus on the detection of suction events from the minimum pump flow,³⁴ of arrhythmic events from the peak-to-peak pump flow frequency,¹⁸ of contractility changes from the pump flow pulse generated,²⁰ or of the open

Address correspondence to Marianne Schmid Daners, Department of Mechanical and Process Engineering, Product Development Group Zurich, ETH Zurich, CLA G 21.1, Tannenstrasse 3, 8092 Zurich, Switzerland. Electronic mail: marischm@ethz.ch

or closed state of the aortic valve from the changes in the pump flow waveform.¹¹ For generating a physiological pump flow, the algorithms developed mainly focused either on adapting the pump flow to the requirements of the patient or on augmenting the arterial pulsatility. Most pump-flow-adaptation controllers developed aim at estimating the preload condition of the LV and adapting the pump flow according to the Frank-Starling mechanism.²⁷ *In-vivo* experiments have proved the outperformance of such controllers against the constant speed operation.²³ The pulsatile operation of a rotary LVAD has been investigated extensively. Amacher *et al.*³ presented the effect of different periodic speed signals and phase shifts to the heart beat on the hemodynamics of an LVAD-assisted pathological circulation. Most of the monitoring and control algorithms proposed are based on a measured or estimated signal which constitutes the input of a simple control structure to achieve one specific objective, e.g., pump flow adaptation.

More complex algorithms which combine various signals and pursue additional objectives have also been presented in literature. For example, Bullister *et al.*⁷ used the pump inlet and outlet pressure and the heart rate as inputs to their pump flow adaptation controller, while they used separate algorithms to detect suction and pump backflow through the estimated pump flow. Arndt *et al.*⁵ used the pressure difference across the pump and developed a control system that responds to preload changes and detects suction events, while it can operate the LVAD in full or partial support. Karantonis *et al.*¹⁴ used the pump-speed signal as input for a classification and regression tree to detect five different states of the LV, i.e., backflow, ventricular ejection, closed aortic valve, and intermittent or continuous suction. Amacher *et al.*¹ presented a more sophisticated approach to compute the optimal waveform of the LVAD speed waveform of for an assisted circulation based on a predefined objective function. For their study, a trade-off function between maximum aortic valve flow and minimum stroke work was applied.

In the current study, we present an advanced control and monitoring system which uses the pump inlet pressure to fulfill the following objectives: (1) To adapt the pump flow to the physiological requirements of the LVAD-supported pathological circulation, (2) to increase the aortic pulse pressure, (3) to ensure an opening of the aortic valve for a predefined period, (4) to provide information regarding the pre- and afterload conditions of the LV as well as the cardiac rhythm, and (5) to ensure the safe operation of the control system, such that no LV suction and overload or pump backflow events occur. As, the various objectives of the algorithms may contradict each other and, therefore, their prioritization approach is being

elaborated. The control system developed was evaluated *in vitro* under several preload, afterload, heart rate, and contractility variations. In the following sections, the *in vitro* performance of the proposed multi-objective control system and its potential for a clinical environment are presented and discussed.

MATERIALS AND METHODS

Hybrid Mock Circulation

Figure 1 depicts the hybrid mock circulation (HMC), where all experiments of the study were conducted. This HMC was earlier developed in our group based on the hardware-in-the-loop (HIL) concept.²¹ It uses a validated numerical model of the human blood circulation⁹ which interacts with a physical LVAD through a hydraulic interface that consists of two pressure reservoirs. The HIL concept works as follows: The LVAD flow is measured by an ultrasound flow probe (TS410/ME-11PXL, Transonic Systems, Ithaca, NY, USA) and is fed into the numerical model. The model computes in real time the LV and the aortic pressures which are then applied through pneumatics at the pressure reservoirs. The new pressures of the hydraulic interface interact with the LVAD and generate an adjusted flow, which follows the same loop path as described above. The numerical model was

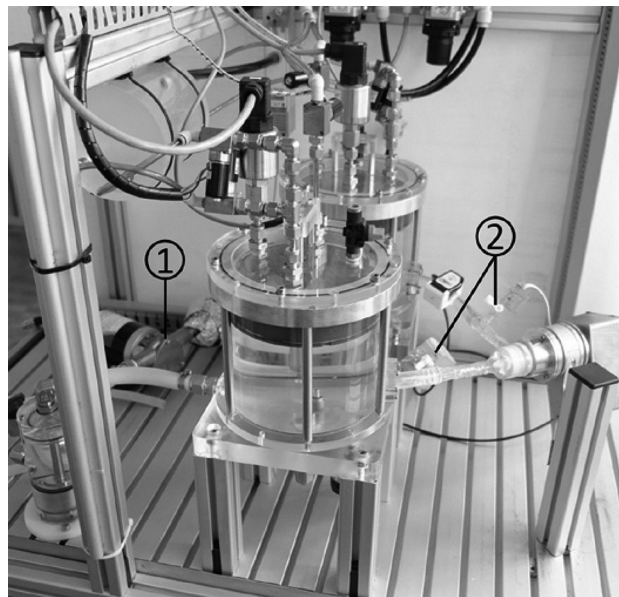


FIGURE 1. Picture of the hybrid mock circulation (HMC) used for the current study. The principle of operation and all components of the HMC were presented in detail by Ochsner *et al.*²¹ Only the reflux pump (1) has been replaced by a flexible impeller pump (Jabsco 18660 Series, Xylem Inc., NY, USA), and pump inlet and outlet disposable pressure transducers (2) (TruWave, Edwards, Lifesciences, Irvine, CA, USA) were added.

TABLE 1. Parameters varied during the experiments of our study. All other parameters of the circulation were fixed and equal for each experiment. The contractility is expressed with respect to the physiological one.

Exp	Description	Time (s)	SVR (mmHg s/mL)	PVR (mmHg s/mL)	UVV (mL)	HR(bpm)	Contractility (%)
1	Preload variation	[0, 20, 25, 80, 90, 120]	1.11	0.1	[2520, 2520, 2020, 2020, 3025, 3025]	80	34
2	Afterload variation	[0, 20, 25, 80, 90, 120]	[1.1, 1.1, 0.51, 0.51, 1.91, 1.91]	0.1	2520	80	34
3	Contractility variation	[0, 20, 25, 80, 90, 120]	1.11	0.1	2520	80	[34, 34, 51, 51, 17, 17]
4	Exercise	[0, 20, 30, 120]	[1.1, 1.1, 0.6, 0.6]	[0.1, 0.1, 0.05, 0.05]	[2520, 2520, 2220, 2220]	[80, 80, 100, 100]	[34, 34, 40, 40]

Exp experiment, *SVR* systemic vascular resistance, *PVR* pulmonary vascular resistance, *UVV* unstressed venous volume, *HR* heart rate.

implemented in MATLAB/Simulink running with Real-Time Windows Target (The Mathworks Inc., Natick, MA, USA) and executed on a PC equipped with two data acquisition boards (MF624 multifunction I/O card, Humusoft s.r.o., Prague, Czech Republic). All signals were recorded at 1 kHz. Instead of a clinical LVAD, we used a non-implantable mixed-flow turbodynamic blood pump, the Deltastream DP2 (Xenios AG, Heilbronn, Germany), which was modified to be controlled as desired. This HMC has been extended to emulate ventricular suction²² as well as to accurately mimic different viscosities.⁶

Experiments

The experiments were split into three main categories. The first category consisted of separate preload, afterload, and contractility variation experiments. The second consisted of an exercise experiment where preload, afterload, heartrate, and contractility vary in parallel. Table 1 summarizes the experiments of these two categories and presents the specific parameters we varied for each of them. For the third category, pre-, afterload, and exercise variations were repeated on circulations with increased and decreased contractility, i.e., 51 and 17%, respectively, with respect to the physiological one, thus mimicking cases of recovery or progression of a heart failure.

Overview of Control System

Figure 2 depicts a schematic overview of the multi-objective physiological control system presented in the current study. It is divided into three main parts (C1–C3) and all main subsystems are enumerated (blocks 1–11). First, the signals used are being processed to filter or add noise and to extract the required features. Then, estimators are implemented, while the part C3 includes all controllers developed. Each enumerated

block includes algorithms which are described in the following subsections and evaluated in the Results section based on the experiments presented in the preceding paragraph.

Signal Processing

Block 1: Low-Pass Filtering Block 1 was implemented to filter the noise from the pump inlet pressure (PIP) signal. The PIP was filtered with a first-order low-pass filter (LPF) with a cut-off frequency of 25 Hz.

Block 2: Feature Extraction Two main indices were extracted from the filtered PIP at every heartbeat, namely the end-diastolic pressure (EDP) and the systolic pressure (SP). In parallel, various features from the PIP and its gradient were extracted to be used for the detection of the state of the aortic valve (block 4) and the MAP estimation (block 5). The features extracted were chosen to depict the different waveforms of the PIP signal with and without aortic valve opening. For our implementation, the systolic phase of the PIP was segmented and the histogram amplitude of each part was used as a feature. Additionally, combinations of the minimum, mean, maximum and root-mean square features were derived from the PIP, as proposed by Ooi *et al.*,²⁴ but with the pump-speed waveform.

Block 3: Minimum Pump Flow Extraction For the current study, the measured pump flow was used to extract the minimum pump flow (block 3). However, in clinical practice the estimated pump flow could be used instead in order to avoid having to use additional sensors. To account for the estimator error, we added a white noise of 0.5 ± 0.2 L/min to the measured pump flow before we fed it to the backflow (part of the safety controller) and speed amplitude controllers.

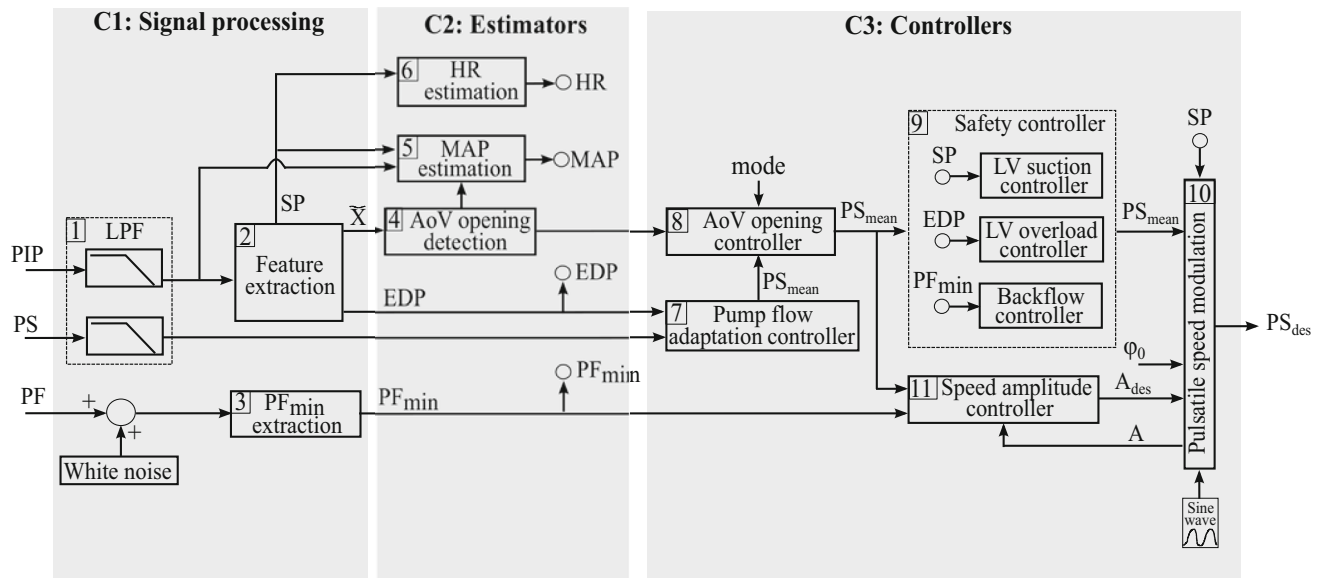


FIGURE 2. Schematic overview of the multi-objective physiological control system proposed in the current study. The input signals of the system are the pump inlet pressure (PIP), the pump speed (PS), and the pump flow (PF). The output is the desired pump speed (PS_{des}). The whole control system is divided into the three main parts named Signal processing (C1), Estimators (C2), and Controllers (C3). Each category consists of the various subsystems illustrated with blocks (1–11). The content of the variable mode is listed in Table 2. LPF low-pass filter, \bar{X} , features extracted from the filtered PIP, SP systolic pressure, EDP end-diastolic pressure, MAP mean aortic pressure, HR heart rate, AoV aortic valve, PF pump flow, *min* minimum, *des* desired, A speed amplitude, and φ_0 phase shift.

Estimators

Block 4: Aortic-Valve-Opening Detection The features extracted in the signal processing (C1, block 2) were used in a linear discrimination algorithm (LDA) to detect the opening state of the aortic valve (block 4). The LDA was based on the minimization of the total probability of misclassifications. This allows a discrimination function to be determined. By assessing the location of a weighted linear combination of the calculated features relative to a threshold, the sample can be classified in indicating either an open or a closed aortic valve. The algorithm was fitted to *in silico* data resulting from Experiments 1 and 2 as listed in Table 1 with a 34% contractility with respect to the physiological one.

Block 5: Mean Aortic Pressure Estimation The mean aortic pressure (MAP) was also estimated for monitoring the afterload of the circulation. To estimate the MAP with the following algorithmic steps, the aortic valve should first be detected as open. Then, based on the PIP gradient, the time close to an aortic valve opening is detected, where the PIP equals the diastolic aortic pressure (AoP_{dias}). Furthermore, as the aortic valve has opened, the SP detected approximates the systolic aortic pressure (AoP_{sys}). Thus, the MAP can be calculated by the known equation $MAP = (2 \cdot AoP_{dias} + AoP_{sys})/3$.

Block 6: Heart Rate Estimation The HR is extracted by calculating the time between two consecutive SP detections (block 6).

Controllers

Block 7: Pump-Flow-Adaptation Controller The last part of the multi-objective physiological control system used the indices extracted from the measured and estimated signals to control the pump speed and generate a physiological pump flow. A purely preload-based approach was used to adapt the pump flow to the requirements of the circulation. The EDP was extracted at every heartbeat and served as an input to a proportional controller, which aims at imitating the linear part of the Frank-Starling curve of the physiological heart.¹² The speed was updated according to the equation

$$PS_{des} = PS_{ref} + (EDP - EDP_{ref}) * K_p \quad (1)$$

where PS_{ref} and EDP_{ref} are the pump speed and EDP values defined during calibration, i.e., when the initial PS is defined, while K_p is the proportional gain which equaled 300 rpm/mmHg. For this purpose, *in vitro* experiments were repeated while increasing the gain stepwise. The very high gains were defined that led to sustained oscillations during a pump speed increase

TABLE 2. Modes of operation of the aortic-valve-opening controller.

Mode	Below PS_{thres}		Above PS_{thres}	
	Open time	Close time	Open time	Close time
1	5 s	15 s	5 s	15 s
2	∞	0	AoV controller deactivated	
3	∞	0	∞	0

The pump speed threshold (PS_{thres}) was set at 4600 rpm for all modes. The symbol ∞ indicates the requirement of a continuously open aortic valve.

and very low gains that led to suction during a pump speed decrease. Then, the final gain was selected such that it differed from the “limit” gains at least by a factor of two. Thus, a good performance against suction was achieved while avoiding oscillations.

Block 8: Aortic-Valve-Opening Controller The knowledge of the state of the aortic valve opening (block 4) was used to adapt the pump speed and influence the state of the aortic valve as desired. The control of the aortic valve opening is based on the user (clinician)-defined open and close thresholds. For example, if the aortic valve is consecutively closed longer than the “closed” threshold, the pump speed is linearly decreased until an aortic valve opening is detected. The pump speed remains low until the aortic valve has opened at least for the time defined by the “open” threshold. The pump speed then returns linearly to the pump speed defined by the pump flow adaptation controller (block 7).

The desired opening time of the aortic valve can lead to quite different responses of the control system presented. For example, assuming a very diseased heart, trying to keep the aortic valve open during exercise conditions may lead to limited perfusion as the heart is not able to pump enough blood through the valve. This condition has been proven clinically by Camboni *et al.*⁸ To prevent such a condition, we added a pump speed threshold ($PS_{thres} = 4600$ rpm, corresponding to an EDP above 13 mmHg) and applied a different objective of the aortic-valve-opening controller above and below this threshold. Therefore, the open and closed times and the PS ranges within which these times apply are adjustable and lead to various modes of operation of the aortic-valve-opening controller (“mode” input variable).

For our study, three different modes were defined and tested under all experiments described in the Experiments section. Table 2 lists these different modes of operation. Mode 1 aims at a regular opening and closing of the valve regardless of the physiological requirements of the circulation. Mode 2 tries to always keep the valve open below the PS_{thres} , whereas it keeps the aortic-valve-opening controller deactivated above

the PS_{thres} . Mode 3 aims at keeping the valve open at all times. In the latter case, the PS was set to operate close to a closing status of the aortic valve to limit the loading of the LV when the valve is open.

Block 9: Safety Controller After the aortic-valve-opening controller, a safety controller (block 9) was implemented that ensures a safe operation by preventing pump speeds that may lead to complications, such as LV suction, LV overload, and pump backflow. For the case of suction, the ratio of negative pressures within a heartbeat, named suction index (SI), is detected and fed into a PI controller ($P = 2500$ rpm/SI, $I = 125$ rpm/SI) that lowers the pump speed to remove the suction event. For the detection and release of LV overload, the EDP measurement is being used. A predefined EDP threshold was set at 20 mmHg to indicate overload. The difference between the measured EDP and the threshold is fed into a PI controller that increases the pump speed to resolve the overload ($P = 250$ rpm/mmHg, $I = 12.5$ rpm/mmHg-s). This controller is only activated after 10 consecutive heartbeats with an EDP above 20 mmHg. To detect and release pump backflow events, the minimum pump flow from block 3 is used. A PI controller with the minimum pump flow as input is implemented to achieve a continuously positive pump flow by increasing the pump speed ($P = 30$ rpm s/ml, $I = 20$ rpm/ml). Anti-reset windup techniques were incorporated to all the PI controllers implemented to prevent overshooting due to accumulated error. All gains were tuned according to the method followed for the pump-flow-adaptation controller to have a safe margin against too high or too low gains.

Block 10: Pulsatile Speed Modulation The last part of the system aimed at increasing the aortic pulse pressure (AoPP). A sinusoidal PS modulation has been implemented that is synchronized to the heartbeat. The synchronization to the heartbeat was based on the SP per heartbeat detection. Based on results from a previous study about the influence of the phase shift on AoPP,³ a co-pulsating mode with a fixed phase shift of 90% (with respect to SP) was applied. The mean value

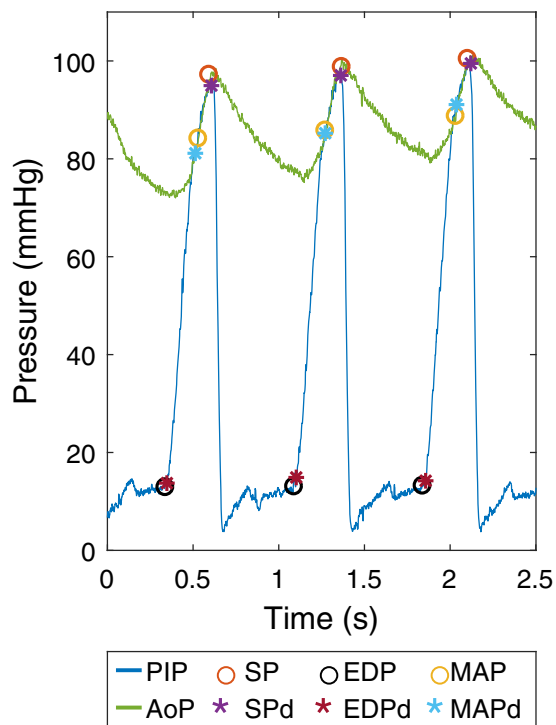


FIGURE 3. Example of detection algorithms during the experiments of the study. The measured signal of pump inlet pressure (PIP) and aortic pressure (AoP) are depicted. The values detected in real-time of the systolic pressure (SPd), the end-diastolic pressure (EDPd), and the mean aortic pressure (MAPd) are indicated by asterisks, while the real values of SP, EDP, and MAP are indicated by circles.

of the sinusoidal waveform was defined by the pump-flow-adaptation controller or the aortic-valve-opening controller.

Block 11: Speed-Amplitude Controller The amplitude of the waveform was controlled such that a positive minimum pump flow was ensured, thus preventing backflow (block 11). An operation close to backflow enabled the maximum AoPP without any possible complications, e.g., blood damage due to backflow. The amount of AoPP achieved depends on the pump characteristics and the contractility of the circulation.

Prioritization of the Controllers

The various controllers included in the multi-objective control system presented call for contrary responses in certain situations, e.g., when for a specific patient condition not all objectives set are met. For example, it may happen that the PS should be greatly decreased to open the aortic valve to the point that backflow may occur. As such cases, may be inevitable where controllers are in conflict with each other, an adjustable prioritizing concept has been

implemented. The safety controller has the first priority, followed by the aortic-valve-opening and the pump-flow-adaptation controllers. By high priority, we define the controller that is most important to define the desired pump speed. If a higher-prioritized controller is active, all lower-prioritized controllers are locked and cannot further influence the mean pump speed. Thus, their output remains the same as the output at the time the higher-prioritized controller became active. This prevents any abrupt speed changes, such as when the speed control changes from the first- to the second-priority controller and back.

The prioritization concept is implemented *via* logic operators. When the safety controller becomes active, it defines the desired pump speed of the LVAD while all other controllers are locked. The locking is implemented by setting the inputs to all other controllers to zero, thus preventing any reaction from these controllers. Compared to a complete deactivation of these controllers, this not only prevents any sudden jump in the desired pump speed, but also any influence from the lower prioritized controllers on the desired speed. Otherwise, the pump speed is defined by the aortic-valve-opening and the pump-flow-adaptation controllers. If the aortic valve status is as desired by the user/clinician, then the pump-flow-adaptation controller regulates the desired pump speed. Else, the aortic-valve-opening controller regulates the pump speed and the pump-flow-adaptation controller is locked.

RESULTS

Signal Processing (C1) and Estimators (C2)

The aortic-valve-opening detection algorithm was evaluated over all the experiments of the study (all three categories described in the Experiments section), such that unseen data are included. Each experiment was executed with all three modes of the AoV opening controller, thus leading to a total of 30 different experiments of 120 s each. The accuracy of the algorithm was 82.33% for the open status and 93.46% for the closed status, while the overall accuracy was 86.35%. Furthermore, the detection of the EDP, SP, HR and the estimation of the MAP were evaluated over the same pool of experiments. The mean absolute errors achieved were: 3.61 mmHg for the EDP, 1.38 mmHg for the SP, 1.86 bpm for the HR and 5.34 mmHg for the MAP. Figure 3 shows an example of the pump inlet and aortic pressures measured over three heartbeats. The values detected during signal processing and the estimated MAP are depicted (asterisks) together with the real values (circles).

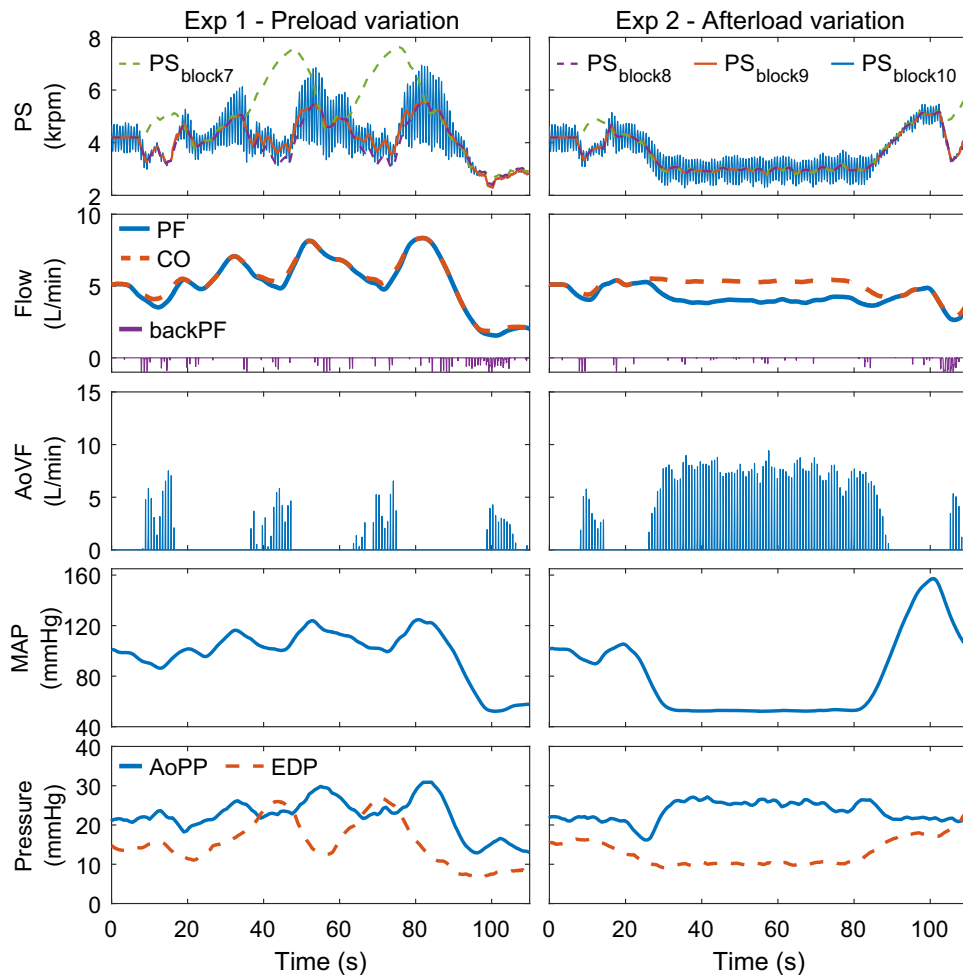


FIGURE 4. Performance results of the multi-objective physiological control system under Experiments (Exp) 1 and 2 (pre- and afterload variations). The aortic-valve-opening controller was operating in Mode 1 (Table 2). The signals of pump speed (PS) and mean PS (\overline{PS}), mean pump flow (\overline{PF}), cardiac output (CO), pump backflow (backPF), aortic valve flow (AoVF), mean aortic pressure (MAP), aortic pulse pressure (AoPP), and end-diastolic pressure (EDP) are depicted. The additional $\overline{PS}_{\text{block},i}$ depicted in the two top panels correspond to the outputs of blocks 7–10 as illustrated in Fig. 2.

Control System

Figure 4 shows the performance of the multi-objective physiological control system during preload and afterload variations. The aortic-valve-opening controller was operated with mode 1. The signals of the pump speed (PS), mean PS (\overline{PS}), mean pump flow (\overline{PF}), cardiac output (CO), pump backflow (backPF), aortic valve flow (AoVF), MAP, AoPP, and EDP are depicted. During preload increase, the \overline{PS} and speed amplitude increased, following the changes of the EDP and leading to a \overline{PF} and MAP increase. However, due to the PS decrease, they all decreased approximately every 15 s, to enable an aortic valve opening, which the positive AoVF clearly shows. During a preload decrease, \overline{PS} decreased due to an EDP decrease and reached the low limit of 2 krpm. This low speed caused backflow and, therefore, the safety controller slightly increased the \overline{PS} after 100 s

to release it. To avoid backflow, the pulsatile speed modulation as well had to be deactivated after 95 s. Some backflow still occurred during the experiment when the speed amplitude was varied.

Additionally, Figure 4 shows the practical implementation of the prioritization concept of the various controllers during the preload variations. Particularly, from 60 to 80 s, the pump-flow-adaptation controller requires a PS increase due to the increased EDP. However, according to user settings, the aortic valve should stay open. As, the aortic-valve-opening controller has a higher priority than the pump-flow-adaptation, this is the one that defines the pump speed. At $t = 65$ s the LV is overloaded, which activates the safety controller (orange line) to overwrite the aortic-valve-opening controller (purple line) and define the \overline{PS} of the pulsatile speed modulation such that the LV overload is released.

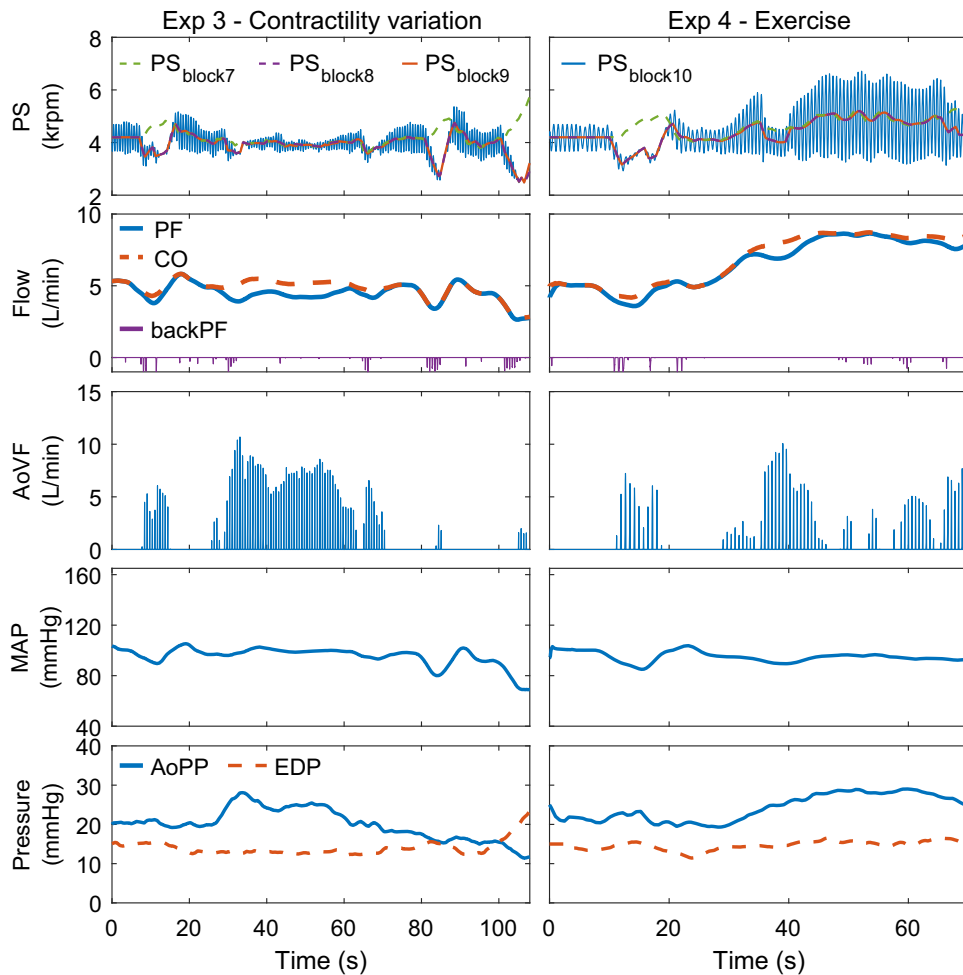


FIGURE 5. Performance results of the multi-objective physiological control system under Experiments (Exp) 3 and 4 (contractility variation and exercise). The aortic-valve-opening controller was operating in Mode 1 (Table 2). The signals of pump speed (PS) and mean PS (\overline{PS}), mean pump flow (PF), cardiac output (CO), pump backflow (backPF), aortic valve flow (AoVF), mean aortic pressure (MAP), aortic pulse pressure (PP), and end-diastolic pressure (EDP) are depicted. The additional $\overline{PS}_{\text{block},i}$ depicted in the two top panels correspond to the outputs of blocks 7–10 as illustrated in Fig. 2.

The afterload decrease caused a strong decrease of the MAP. The \overline{PS} and \overline{PF} in turn decreased due to the EDP decrease. Despite that, the CO remained unchanged as the AoVF increased, which yielded an AoPP of around 28 mmHg. The afterload increase increased the MAP and the EDP. Thus the \overline{PS} and the \overline{PF} increased according to the actions of the pump-flow-adaptation controller. The \overline{PF} increase led to an aortic valve closure and the CO decreased slightly. At $t = 100$ s, the \overline{PS} started to decrease to enable an aortic valve opening, as it remained closed for more than 15 s (mode 1). For both experiments, the green, purple, red, and blue \overline{PS} signals show how differently the pump-flow-adaptation controller, the aortic-valve-opening controller, the safety controller, and the pulsatile speed modulation, respectively, control the PS during the experiments.

Figure 5 presents the same signals as Figure 4, but for Experiments 3 and 4 listed in Table 1. During a

contractility increase (Exp 3) after $t = 20$ s, the \overline{PS} slightly decreased due to the EDP decrease, while the pulsatile speed modulation was operated with a decreased speed amplitude to prevent backflow. At the same time, the AoVF and AoPP increased while the MAP and CO remained unchanged. When contractility decreased, the LVAD support increased by increasing the \overline{PS} and \overline{PF} , while the speed amplitude of the pulsatile speed modulation was increased. At approximately $t = 80$ s and $t = 100$ s, a prolonged aortic valve closure was detected that led to an LVAD support decrease such that the valve opened, which in turn yielded an EDP greater than 20 mmHg. During exercise, due to the preload increase, the LVAD support increased by increasing the \overline{PS} , the \overline{PF} , and the speed amplitude of the pulsatile speed modulation. Thus, the CO and AoPP increased at 8 L/min and 28 mmHg, respectively, whereas the MAP and EDP

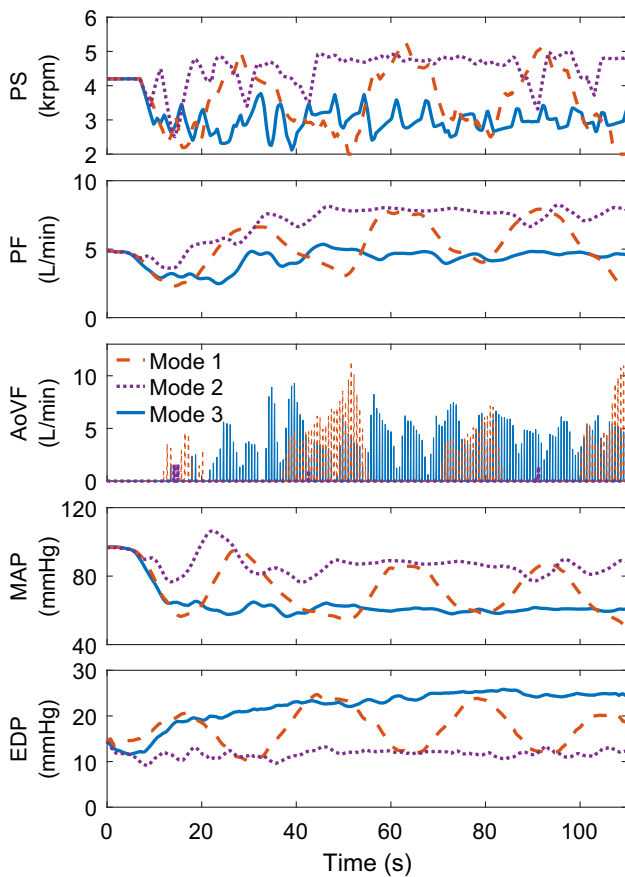


FIGURE 6. Performance results of the multi-objective physiological control system under Experiment 4 (exercise) with a decreased contractility of 17% and when the aortic-valve-opening controller is operated with each of the three modes (Table 2). The signals of mean pump speed (\overline{PS}), mean pump flow (\overline{PF}), aortic valve flow (AoVF), mean aortic pressure (MAP), and end-diastolic pressure (EDP) are shown.

remained unchanged. The aortic valve never stayed closed for more than 15 s during exercise. Therefore, no regular reduction in the \overline{PS} was recorded. If the circulation settings would return to their initial values of resting conditions, the physiological control system would restore the hemodynamics as well. Results that prove this ability of the control system presented are provided within the supplementary material.

Figure 6 shows the various performance effects of the multi-objective physiological control system during the exercise experiment, but when an LVAD was regulated which supports a circulation whose contractility decreased from 34 to 17%. The experiment was repeated while operating the aortic-valve-opening controller in all three modes of the aortic-valve-opening controller (Table 2). The signals of \overline{PS} , \overline{PF} , AoVF, MAP, and EDP are depicted for each mode. With Mode 1, a regular opening of the aortic valve was achieved. During exercise ($t > 20$ s), the \overline{PS} , the \overline{PF} and the MAP in turn dropped (between approximately

$t \in [30, 50]$ s, $[65, 80]$ s and $[95, 110]$ s) to let the valve open, leading to an EDP above 20 mmHg for a few seconds. When the valve stayed closed, a \overline{PF} of approximately 8 L/min resulted, whereas during the time of an opened aortic valve the \overline{PF} dropped below 5 L/min. With Mode 2, the valve status was not controlled during exercise, as the desired \overline{PS} of the pump flow adaptation controller was above the given $\overline{PS}_{\text{thres}}$. This mode yielded the higher \overline{PF} and MAP among all modes, while it kept the EDP at around 11 mmHg.

Finally, with Mode 3, the valve status was controlled such as to stay always open during the whole experiment, thus leading to an EDP above 20 mmHg during exercise ($t > 20$ s). For this case, the LV overload controller of the safety controller was deactivated in order to better observe the influence of Mode 3 on the EDP. Despite the high EDP, the \overline{PS} did not increase, as it would due to the pump flow adaptation controller, in order to keep the aortic valve open (according to our prioritization). The abrupt \overline{PS} increase and decrease were due to the effort of the multi-objective controller to operate slightly above the \overline{PS} that leads to a closed valve, i.e., to keep the aortic valve open while avoiding an overload of the LV. Despite these \overline{PS} changes, the \overline{PF} remained almost unchanged except below 5 L/min. The limited perfusion led to very low values of MAP of 60 mmHg.

DISCUSSION

The current study presents a novel, multi-objective, physiological control system, which, to our knowledge, is the first to incorporate the described functionalities based on a single pressure sensor alone at the inlet of an LVAD. Here, the DP2 was used as an LVAD, but the control system can be implemented in any clinical rotary LVAD after adapting the gains. The controller has been extensively evaluated *in vitro* and has met the set requirements during preload, afterload, and contractility variations. The \overline{PS} was regulated such that it adapts to varying physiological requirements, augments the AoPP, and enables a controlled aortic valve opening. It was surrounded by algorithms that provided important indices for the monitoring of a pathological circulation assisted by an LVAD, such as the status of the aortic valve, the afterload conditions, and the cardiac rhythm. Safety features were implemented to ensure a safe operation by overwriting and compensating any failures of the control system. Thus, no suction events occurred, which was not the case during the same pre- and afterload decrease experiments with a constant speed LVAD, as previously presented by Petrou *et al.*²⁶ A prioritization concept

was successfully implemented to switch among the different controllers. The pump speed signals in Figs. 4 and 5 show the effect of this prioritization.

In our system, an EDP-based pump flow adaptation controller was used. This approach is highly intuitive when it is used to aim at imitating the Frank-Starling mechanism. A similar approach with a proportional controller was presented by Kwan-Gett *et al.*¹⁶ many years ago, but it was based on the measurement of the left atrial pressure (LAP). A preload-based pressure-control system was recently presented by Stevens *et al.*³¹ and Mansouri *et al.*,¹⁷ but they used EDP together with pump flow. Bullister *et al.*⁷ used the minimum diastolic pressure as an input for a physiological controller, but their approach required the pump outlet pressure data as well. Another preload-based pump flow adaptation controller, which uses the end-diastolic volume, was developed by Ochsner *et al.*²² The benefit of preload-based controllers had been described by Tchanchaleishvili *et al.*³² and was proven *in vitro* by Pauls *et al.*²⁵ as well as *in vivo* by Ochsner *et al.*²³

A feedback controller that is more dynamic for pulsatile speed modulation is presented here. Thus far, all studies that presented pulsatile speed modulation algorithms were based on feedforward approaches and were mainly investigating the influences of phase shift and amplitude.³ To our knowledge, no experiments under varying physiological requirements have been presented that operate the LVAD in a pulsatile mode. The feedforward approach may lead to backflow when PS is not high enough to overcome the afterload conditions, especially if the LVAD design leads to flat pump characteristics. Ando *et al.*⁴ proposed the counterpulsation as a method to avoid backflow, but it limits the potential increase in AoPP. In the control system presented, we dynamically vary the parameters of the periodic speed waveform and thus achieve the maximum possible AoPP, which here is three times higher than without pulsatile speed modulation, while we limit the negative effects. Despite the backflows observed (Figs. 4, 5), which resulted from the overshoot of the speed-amplitude controller, the performance can be improved by increasing the desired reference minimum pump flow, for instance. Furthermore, we showed that by using the PIP, we can robustly synchronize the pump speed with the heartbeat, while up to now, ECG was the main approach for synchronization.²

Despite the effort to increase the AoPP, the authors acknowledge that the amount of pulsatility required and its positive effects remain controversial.²⁸ Furthermore, an AoPP increase alone cannot guarantee improved hemodynamics, while there are additional indices that need to be investigated, such as the gra-

dient of the AoPP.³³ However, the proposed control system may constitute the basis for a reliable system that can support the efforts to answer the questions concerning the required pulsatility and its benefits without inducing any new problems, such as additional blood damage due to backflow.³³

Various approaches to detect an aortic valve opening have been proposed in literature. Ooi *et al.*²⁴ used the pump speed to detect a non-opening state, whereas Granegger *et al.*¹¹ used the estimated pump flow to detect the state of the aortic valve. Jansen-Park *et al.*¹³ presented an invasive approach to detect the pump speed that leads to aortic valve closure based on the pump inlet pressure and the pump power. Granegger *et al.*¹¹ evaluated their approach even clinically, but with stable hemodynamics. None of these approaches have been evaluated under varying physiological requirements and with contractility changes or together with a pump-flow-adaptation controller. Although the idea of an aortic-valve-opening controller had been proposed earlier, here we present the performance of such a system that would allow the clinician to predefine the opening time of the valve together with additional controllers, such as the pump-flow-adaptation controller.

The opening of the aortic valve constitutes a crucial condition for the LVAD patients as it can prevent aortic valve insufficiency and decrease the possibility of thrombogenicity at the aortic root.¹⁰ Furthermore, a switch of the LVAD operation such that it closes or opens the aortic valve can be related to a switch between maximum unloading to decrease the stroke work, to increase the loading of the LV, and to allow a gradual training of the heart muscle. In other words, such a control system would ensure that the patient remains in full or partial support as desired by the clinician. Thus, the risk of myocardial atrophy could be reduced and methods towards the myocardial recovery could be established.

Most of the physiological controllers proposed use gains which have been determined for a specific *in vitro* circulation. An inappropriate gain due to interpatient variability may lead to values of PS that are too high and, therefore, cause aortic valve closure or even LV suction. Furthermore, backflow or even LV overload may occur when the PS is set too low. The novel, multi-objective, physiological control system presented considers such events and constitutes a potential system for a robust performance even among various circulations.

Limitations

The authors acknowledge that the current study contains certain limitations, which would need to be

addressed in the future. (1) So far, no reliable, long-term blood pressure sensor for VADs is available. However, much research is currently in progress in this area and promising results have been presented in literature.^{30,32} Therefore, it is reasonable to investigate the possible benefits of the usage of such a sensor. (2) We applied a white noise to the measured pump flow instead of using an estimator. Pump-flow estimators have already been described extensively in literature and are being used clinically (e.g., Heartmate 3, Abbott Laboratories Inc.). To avoid increasing the size and complexity of the manuscript we preferred not to include such an estimator within the control system presented. (3) Abrupt speed changes resulted from the proposed control system. It can be questionable how these speed accelerations influence the potential blood damage. However, state-of-the-art devices, such as the Heartmate 3, have implemented algorithms in clinical practice that cause fast speed changes to induce wash-out. (4) The implementation of the MAP estimator cannot be accurate during full support, i.e., when the aortic valve is continuously closed. It can be used only during a detected aortic valve opening. (5) The accuracy of the aortic-valve-opening algorithm in a clinical environment should be investigated further. Thus far, a clinical study has shown promising results for such an algorithm,¹¹ while in our study the accuracy was sufficient even during changes of the physiological requirements and the contractility of the circulation. However, cases with mitral or aortic valve insufficiencies should also be considered as they may influence the accuracy of the algorithm. To account for such possible limitations and present a fail-safe behavior, a safety controller such as the one included in our control system is crucial, especially in a clinical environment.

CONCLUSION

The latest technological improvements promise the integration of a pressure sensor in an LVAD. This will broaden the possibilities for controlling the LVAD and monitoring the LVAD-supported pathological circulation. The current study shows the potential of the novel, multi-objective physiological control system developed that only uses the signal of a pressure sensor at the pump inlet, to control the speed of an LVAD. *In-vitro* results showed that our control system can adapt the pump flow to varying physiological requirements, increase the aortic pulse pressure, regulate the opening of the aortic valve, and ensure a safe operation while offering important hemodynamic variables for monitoring the circulation. To our knowledge, no physiological control system that serves

for all these objectives has been presented in literature up to now. As a next step, *in vivo* experiments would be required to further evaluate and improve these algorithms.

ELECTRONIC SUPPLEMENTARY MATERIAL

The online version of this article (doi: [10.1007/s10439-017-1919-0](https://doi.org/10.1007/s10439-017-1919-0)) contains supplementary material, which is available to authorized users.

ACKNOWLEDGMENTS

The authors gratefully acknowledge the financial support by the Stavros Niarchos Foundation. This work is part of the Zurich Heart project under the umbrella of University Medicine Zurich.

REFERENCES

- ¹Amacher, R., J. Asprion, G. Ochsner, H. Tevaearai, M. J. Wilhelm, A. Plass, A. Amstutz, S. Vandenberghe, and M. Schmid Daners. Numerical optimal control of turbo dynamic ventricular assist devices. *Bioengineering* 1:22–46, 2013.
- ²Amacher, R., G. Ochsner, A. Ferreira, S. Vandenberghe, and M. Schmid Daners. A robust reference signal generator for synchronized ventricular assist devices. *IEEE Trans. Biomed. Eng.* 60:2174–2183, 2013.
- ³Amacher, R., G. Ochsner, and M. Schmid Daners. Synchronized pulsatile speed control of turbodynamic left ventricular assist devices: review and prospects. *Artif. Organs* 38:867–875, 2014.
- ⁴Ando, M., Y. Takewa, T. Nishimura, K. Yamazaki, S. Kyo, M. Ono, T. Tsukiya, T. Mizuno, Y. Taenaka, and E. Tatsumi. A novel counterpulsation mode of rotary left ventricular assist devices can enhance myocardial perfusion. *Int. J. Artif. Organs* 14:185–191, 2011.
- ⁵Arndt, A., P. Nüsser, and B. Lampe. Fully autonomous preload-sensitive control of implantable rotary blood pumps. *Artif. Organs* 34:726–735, 2010.
- ⁶Boës, S., G. Ochsner, R. Amacher, A. Petrou, M. Meboldt, and M. Schmid Daners. Control of the fluid viscosity in a mock circulation. *Artif. Organs*, 2017. doi: [10.1111/aor.12948](https://doi.org/10.1111/aor.12948).
- ⁷Bullister, E., S. Reich, and J. Sluetz. Physiologic control algorithms for rotary blood pumps using pressure sensor input. *Artif. Organs* 26:931–938, 2002.
- ⁸Camboni, D., T. J. Lange, P. Ganslmeier, S. Hirt, B. Flörchinger, Y. Zausig, L. Rupprecht, M. Hilker, and C. Schmid. Left ventricular support adjustment to aortic valve opening with analysis of exercise capacity. *J. Cardiothorac. Surg.* 9:93, 2014.
- ⁹Colacino, F. M., F. Moscato, F. Piedimonte, M. Arabia, and G. A. Danieli. Left ventricle load impedance control by apical vad can help heart recovery and patient perfusion: a numerical study. *ASAIO J.* 53:263–277, 2007.

- ¹⁰Crestanello, J. A., D. A. Orsinelli, M. S. Firstenberg, and C. Sai-Sudhakar. Aortic valve thrombosis after implantation of temporary left ventricular assist device. *Interact. Cardiovasc. Thorac. Surg.* 8:661–662, 2009.
- ¹¹Granegger, M., M. Masetti, R. Laohasurayodhin, T. Schloeglhofer, D. Zimpfer, H. Schima, and F. Moscato. Continuous monitoring of aortic valve opening in rotary blood pump patients. *IEEE Trans. Biomed. Eng.* 63:1201–1207, 2016.
- ¹²Guyton, A. C. Textbook of medical physiology. *Acad. Med.* 36:556, 1961.
- ¹³Jansen-Park, S.-H., S. Spiliopoulos, H. Deng, N. Greatrex, U. Steinseifer, D. Guersoy, R. Koerfer, and G. Tenderich. A monitoring and physiological control system for determining aortic valve closing with a ventricular assist device. *Eur. J. Cardiothorac. Surg.* 46:356–360, 2014.
- ¹⁴Karantonis, D. M., E. Lim, D. G. Mason, R. F. Salamonsen, P. J. Ayre, and N. H. Lovell. Noninvasive activity-based control of an implantable rotary blood pump: comparative software simulation study. *Artif. Organs* 34:E34–E45, 2010.
- ¹⁵Kirklin, J. K., D. C. Naftel, F. D. Pagani, R. L. Kormos, L. W. Stevenson, E. D. Blume, S. L. Myers, M. A. Miller, J. T. Baldwin, and J. B. Young. Seventh INTERMACS annual report: 15,000 patients and counting. *J. Heart Lung Transplant.* 34:1495–1504, 2015.
- ¹⁶Kwan-Gett, C., M. Crosby, A. Schoenberg, S. Jacobsen, and W. Kolff. Control systems for artificial hearts. *ASAIO J.* 14:284–290, 1968.
- ¹⁷Mansouri, M., R. F. Salamonsen, E. Lim, R. Akmeliawati, and N. H. Lovell. Preload-based starling-like control for rotary blood pumps: numerical comparison with pulsatility control and constant speed operation. *PLoS ONE* 10:e0121413, 2015.
- ¹⁸Moscato, F., M. Granegger, M. Edelmayer, D. Zimpfer, and H. Schima. Continuous monitoring of cardiac rhythms in left ventricular assist device patients. *Artif. Organs* 38:191–198, 2014.
- ¹⁹Moscato, F., M. Granegger, P. Naiyanetr, G. Wieselthaler, and H. Schima. Evaluation of left ventricular relaxation in rotary blood pump recipients using the pump flow waveform: a simulation study. *Artif. Organs* 36:470–478, 2012.
- ²⁰Naiyanetr, P., F. Moscato, M. Vollkron, D. Zimpfer, G. Wieselthaler, and H. Schima. Continuous assessment of cardiac function during rotary blood pump support: a contractility index derived from pump flow. *J. Heart Lung Transplant.* 29:37–44, 2010.
- ²¹Ochsner, G., R. Amacher, A. Amstutz, A. Plass, M. S. Daners, H. Tevaearai, S. Vandenberghe, M. J. Wilhelm, and L. Guzzella. A novel interface for hybrid mock circulations to evaluate ventricular assist devices. *IEEE Trans. Biomed. Eng.* 60:507–516, 2013.
- ²²Ochsner, G., R. Amacher, M. J. Wilhelm, S. Vandenberghe, H. Tevaearai, A. Plass, A. Amstutz, V. Falk, and M. Schmid Daners. A physiological controller for turbodynamic ventricular assist devices based on a measurement of the left ventricular volume. *Artif. Organs* 38:527–538, 2013.
- ²³Ochsner, G., M. J. Wilhelm, R. Amacher, A. Petrou, N. Cesarovic, S. Staufert, B. Röhrnbauer, F. Maisano, C. Hierold, M. Meboldt, *et al.* In vivo evaluation of physiological control algorithms for LVADs based on left ventricular volume or pressure. *ASAIO J.* 63:568–577, 2017.
- ²⁴Ooi, H.-L., S.-C. Ng, E. Lim, R. F. Salamonsen, A. P. Avolio, and N. H. Lovell. Robust aortic valve non-opening detection for different cardiac conditions. *Artif. Organs* 38:E57–E67, 2014.
- ²⁵Pauls, J. P., M. C. Stevens, N. Bartnikowski, J. F. Fraser, S. D. Gregory, and G. Tansley. Evaluation of physiological control systems for rotary left ventricular assist devices: an in vitro study. *Ann. Biomed. Eng.* 44:2377–2387, 2016.
- ²⁶Petrou, A., G. Ochsner, R. Amacher, P. Pergantis, M. Rebholz, M. Meboldt, and M. Schmid Daners. A physiological controller for turbodynamic ventricular assist devices based on left ventricular systolic pressure. *Artif. Organs* 40:842–855, 2016.
- ²⁷Salamonsen, R. F., E. Lim, N. Gaddum, A.-H. H. Aiomari, S. D. Gregory, M. Stevens, D. G. Mason, J. F. Fraser, D. Timms, M. K. Karunanithi, *et al.* Theoretical foundations of a starling-like controller for rotary blood pumps. *Artif. Organs* 36:787–796, 2012.
- ²⁸Schima, H., K. Dimitrov, and D. Zimpfer. Debate: creating adequate pulse with a continuous flow ventricular assist device: can it be done and should it be done? probably not, it may cause more problems than benefits!. *Curr. Opin. Cardiol.* 31:337–342, 2016.
- ²⁹Schmid Daners, M., F. Kaufmann, R. Amacher, G. Ochsner, M. J. Wilhelm, A. Ferrari, E. Mazza, D. Poulikakos, M. Meboldt, and V. Falk. Left ventricular assist devices: challenges toward sustaining long-term patient care. *Ann. Biomed. Eng.* 45:1836–1851, 2017.
- ³⁰Staufert, S., and C. Hierold. Novel sensor integration approach for blood pressure sensing in ventricular assist devices. *Procedia Eng.* 168:71–75, 2016.
- ³¹Stevens, M. C., N. R. Gaddum, M. Percy, R. F. Salamonsen, D. L. Timms, D. G. Mason, and J. F. Fraser. Frank-starling control of a left ventricular assist device. In: *Conf Proc IEEE Eng Med Biol Soc*, pp. 1335–1338, IEEE 2011.
- ³²Tchanchaleishvili, V., J. G. Luc, C. M. Cohan, K. Phan, L. Hübbert, S. W. Day, and H. T. Massey. Clinical implications of physiological flow adjustment in continuous-flow left ventricular assist devices. *ASAIO J.* 63:214–250, 2017.
- ³³Ündar, A. Myths and truths of pulsatile and nonpulsatile perfusion during acute and chronic cardiac support. *Artif. Organs* 28:439–443, 2004.
- ³⁴Vollkron, M., H. Schima, L. Huber, R. Benkowski, G. Morello, and G. Wieselthaler. Development of a reliable automatic speed control system for rotary blood pumps. *J. Heart Lung Transplant.* 24:1878–1885, 2005.